

# REconfigurable Terahertz INtegrated Architecture (RETINA)

Stepan Lucyszyn and Yun Zhou  
Imperial College London, London, SW7 2AZ, United Kingdom

**Abstract**—A paradigm shift in the way millimetre-wave components and subsystems are conceived is presented with our **REconfigurable Terahertz INtegrated Architecture (RETINA)** concept. Here, an entirely new way of implementing **virtual metal-pipe rectangular waveguides** is demonstrated through simulations. Instead of having traditional air-filled structures with solid metal sidewalls, waveguides have **photo-induced virtual sidewalls within high resistivity silicon**. This new technology allows components to be tunable and subsystems to be reconfigurable, by changing light source patterns. A summary of the detailed analysis of wall photoconductivity and electromagnetic simulations is presented here for the first time.

## I. INTRODUCTION AND BACKGROUND

The ability to control subsystem building blocks within a front-end architecture, by electronic means, is important if the overall system is to be adaptive or requires multi-functionality. Techniques for achieving this are well established at microwave [1] and optical frequencies. However, for low loss circuits operating at upper-millimetre-wave and sub-millimetre-wave frequencies (e.g. *circa* 100 to 300 GHz) rectangular waveguides represent the only realistic form of guided-wave structure.

With the RETINA concept, the two sidewalls of a traditional metal-pipe rectangular waveguide (MPRWG) [2] are replaced by regions made conductive by the photo-generation of free carriers. Photoconductivity (PC) within semiconductors and other materials has been known and exploited for many decades [3]. Applications include: optical detectors [4]; sub-picosecond switches [5-6]; optically controlled microwave devices [7-8]; and experimental Bragg reflecting filters [9]. In all cases, the photo-induced electro-hole pair plasma region is confined to the surface of the semiconductor.

In contrast, with reference to Fig. 1, RETINA relies on the photo-induced plasma being extended from the top surface downwards towards the bottom surface of the semiconductor.

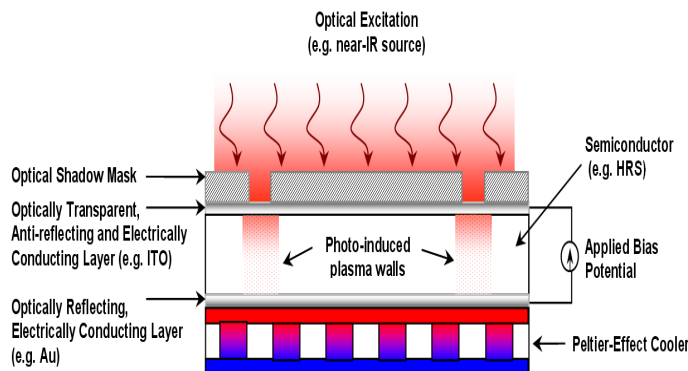


Fig. 1. Simplified illustration of the basic RETINA concept to create a *virtual* MPRWG.

Fig. 1 shows the cross-section of a *virtual* MPRWG, created using the basic RETINA concept. The top surface of the waveguide can be made from indium tin oxide (ITO) or another transparent conductive oxide (TCO). TCO materials have a relatively low plasma frequency, making them transparent within the near-infrared (IR) parts of the frequency spectrum. As a result, they exhibit low attenuation of light from a near-IR laser source, while providing excellent confinement at low terahertz frequencies. Moreover, with a quarter-wavelength thickness (e.g. approximately 0.4  $\mu\text{m}$  for ITO with an 808 nm source), they can also act as anti-reflecting coatings. The bottom layer of the waveguide can be made from gold, so simplicity.

## II. SIMULATION RESULTS

Photoconductivity is the increase in the electrical conductivity of a material caused by incident electromagnetic radiation [3]. In theory, a single photon can generate an electron-hole pair, provided its energy exceeds the band gap energy ( $E_g$ ) of the material. In order for this to occur the radiation source should have a wavelength,  $\lambda_{op} \leq hc / E_g$ , where  $h$  is Planck's constant and  $c$  is the speed of light in vacuo, or, equivalently,  $\lambda_{op} [\mu\text{m}] \leq 1.24 / E_g [eV]$ .

The feasibility of the RETINA concept has been investigated using commercial optoelectronic device simulation software *Silvaco<sup>TM</sup> Luminous* and high frequency structure simulation software *ANSOFT HFSS<sup>TM</sup>*. Figs. 2 show results from *Luminous*, focusing on the photo-induced carrier profiles. Here, a 100  $\mu\text{m}$  thick HRS wafer is exposed by two independent light sources of 808 nm wavelength, each modelled as a normally incident plane wave truncated to an area of 50 x 3,400  $\mu\text{m}^2$  at the ITO surface. The total power of each source is 136 mW, giving an incident power density of 80  $\text{W}/\text{cm}^2$  at the top surface of the ITO layer. The 2D contour profile of the resulting photo-induced total (electron and hole) current density is shown in Fig. 2, with an additional bias potential of +0.1 V between the ITO and gold layers.

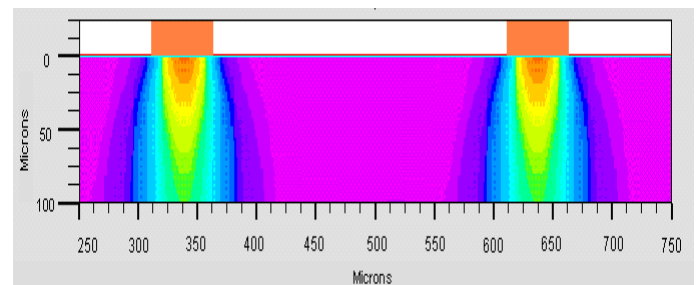


Fig. 2. Simulated (*Luminous*) cross-section of steady-state photo-induced total current density

When a continuous wave (CW) optical source is applied homogeneously along the MPRWG's *virtual wall*, using data provided by *Luminous*, it is possible to extract the equivalent photoconductivity. This information can then be discretized into a matrix of multiple columns and rows, as shown in Fig. 3(a), so that a *virtual MPRWG* can be simulated using *HFSS<sup>TM</sup>*. With this simplified approach, having seven levels of vertical and horizontal photoconductivity, the results from electromagnetic simulations are shown in Fig. 3(b) and (c).

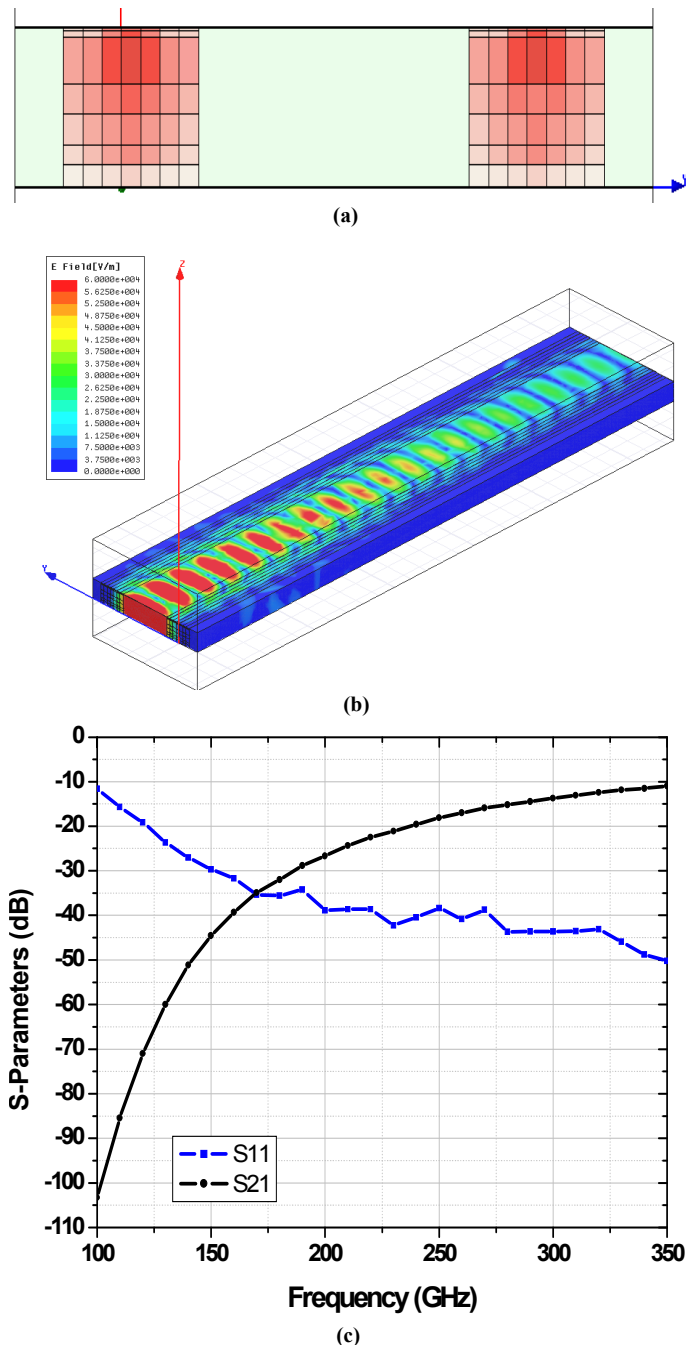


Fig. 3. 3D electromagnetic (*HFSS<sup>TM</sup>*) simulation of a 300 GHz RETINA waveguide ( $10 \lambda_g$  in total length): (a) discretized photoconductivity cross-sectional profile (spatially non-uniform  $7 \times 7$  matrix for each beam); (b) E-field distribution, indicating no side leakage of energy; (c) S-parameter frequency responses.

With  $8 \text{ k}\Omega\cdot\text{cm}$  HRS having a dielectric constant and loss tangent of 12.86 and  $6 \times 10^{-4}$ , respectively at 300 GHz [10], the maximum photoconductivity region has a value of only 2,898 S/m. The gold layer is  $1 \mu\text{m}$  thick in both *Luminous* and *HFSS<sup>TM</sup>* simulations. From Fig. 3(c), the RETINA waveguide is predicted to have an insertion loss of 1.37 dB/ $\lambda_g$ . This result can be compared with 0.04 dB/ $\lambda_g$  at only 100 GHz for an air-filled MPRWG realized using a two-wafer silicon bulk micromaching process [11].

### III. CONCLUSIONS

In this paper, the novel RETINA concept has been reported for the first time. While the RETINA waveguide has much more loss than an air-filled micromachined MPRWG, the flexibility of being able to implement reconfigurable integrated architectures and tunable circuits at terahertz frequencies is a very important advantage. With further optimization in the choice of architectures, materials used, optical source (wavelength, power density and beam profile) and applied bias potential, considerable improvements in the future performance of RETINA's *virtual MPRWGs* can be expected.

With the paradigm shift in the way that reconfigurable integrated architecture are conceived, RETINA offers the possibility of implementing new applications at terahertz frequencies.

### REFERENCES

- [1] S. Lucyszyn and I. D. Robertson, "Analog reflection topology building blocks for adaptive microwave signal processing applications", *IEEE Trans. on Micro. Theory Tech.*, vol. MTT-43, no. 3, pp. 601-611, Mar. 1995.
- [2] S. Lucyszyn, D. Budimir, Q. H. Wang and I. D. Robertson, "Design of compact monolithic dielectric-filled metal-pipe rectangular waveguides for millimetre-wave applications", *IEE Proceedings - Microwaves, Antennas and Propagation*, vol. 143, no. 5, pp. 451-453, Oct. 1996
- [3] A. Ambroziak, "Semiconductor Photoelectric Devices", Iliffe Books. London, 1968
- [4] N. V. Joshi, "Photoconductivity: art, science and technology", New York: Marcel Dekker, 1990
- [5] A. M. Johnson and D. H. Auston, "Microwave switching by picosecond photoconductivity", *IEEE J. of Quantum Electronics*, vol. QE-11, no. 6, pp. 283-287, Jun. 1975
- [6] C. H. Lee, "Picosecond optoelectronic switching in GaAs", *Appl. Phys. Lett.*, vol. 30, no. 2, pp. 84-86, Jan. 1977
- [7] A. J. Seeds and A. A. De Salles, "Optical control of microwave semiconductor devices", *IEEE Transactions on Microwave Theory Tech.*, vol. 38, no. 5, pp. 577-585, May 1990
- [8] S. N. Afsar and I. D. Robertson, "Optically-induced measurement anomalies with voltage-tunable analog control MMICs", *IEEE Transactions on Microwave Theory Tech.*, vol. 46, no. 8, pp. 1105-1114, Aug. 1998
- [9] W. Platte, "LED-induced distributed Bragg reflection microwave filter with fibre-optically controlled change of center frequency via photoconductivity grating", *IEEE Transactions on Microwave Theory Tech.*, vol. 39, no. 2, pp. 359-363, Feb. 1991
- [10] M. N. Afsar and K. J. Button, "Precise millimeter-wave measurements of complex refractive index, complex dielectric permittivity and loss tangent of GaAs, Si, SiO<sub>2</sub>, Al<sub>2</sub>O<sub>3</sub>, BeO, Macor and Glass", *IEEE Trans. Microwave Theory Tech.*, vol. 31, no. 2, pp. 217-223, Feb. 1983.
- [11] W. R. McGrath, C. Walker, M. Yap, and Y-C Tai, "Silicon micromachined waveguides for millimeter-wave and submillimeterwave frequencies", *IEEE Microw. Guid. Wave Lett.*, vol. 3, no. 3, pp. 61-63, 1993